

# Nucleation and crystallization of polypropylene by mineral fillers: relationship to impact strength

P. M. McGenity, J. J. Hooper, C. D. Paynter, A. M. Riley, C. Nutbeem, N. J. Elton and J. M. Adams\*

ECC International Ltd, John Keay House, St Austell, Cornwall PL25 4DJ, UK  
(Received 10 February 1992; accepted 17 March 1992)

The mechanical properties of mineral-filled polypropylene (PP) are determined not only by the size, shape and modulus of the filler particles, but also by microstructure. For example, poor impact strength is correlated with a high capacity for nucleation of crystallization. In the present study, optical microscopy has been used to measure the growth rate of spherulites in PP. In tandem with this, isothermal d.s.c. measurements have been made of the crystallization of the PP filled with talc, calcium carbonate and stearate-coated carbonate at different loading levels. Computer simulation of spherulite growth has been used to derive the number of nucleating sites per unit volume of polymer and, using surface area measurements, the number of sites per unit area of mineral surface was obtained. Values for talc were, as expected, considerably higher than those for carbonate (and especially coated carbonate) fillers. The presence of filler affects not only the nucleation and kinetics of the crystallization process but also the crystallinity and orientation indices and the proportion of  $\beta$ -phase crystallites present. The connection between these factors and impact strength is discussed. It is concluded that impact properties are determined by *inter alia* crack pinning and blocking by filler particles, stress concentrations at the edges of the filler particles, and the nucleating ability of the filler.

(Keywords: polypropylene; spherulites; nucleating sites; talc; calcium carbonate)

## INTRODUCTION

The original purpose of adding mineral fillers to polymers was one of cost reduction. However, more recently, fillers have been used increasingly to fulfil functional roles, such as enhancing stiffness, decreasing electrical loss or increasing absorption of i.r. radiation.

If we concentrate on polypropylene (PP), we note that talc and calcium carbonate are the fillers normally employed in Europe, though small amounts of mica and wollastonite are also used<sup>1</sup>. Primarily, the properties of interest are mechanical. In principle, fillers can modify the mechanical characteristics of a polymer in two ways. First, the properties of the particles themselves (size, shape, modulus) have a direct effect while, second, the presence of filler particles can lead to changes in micromorphology which may give rise to differences in observed bulk properties.

The attention which has been given to the calculation of elastic moduli of heterogeneous systems has resulted in a reasonable qualitative understanding of the topic. Moduli can be predicted fairly well from a knowledge of the moduli of the filler and polymer, the aspect ratio of the filler and the loading level<sup>2-6</sup>. Further progress towards a full quantitative understanding of this area is likely to be reached in the foreseeable future.

If we consider impact strength, however, we find a much lower level of predictive ability. The relevance of the Griffith flaw theory<sup>7</sup> to filled polymers has been fully

confirmed, not least by Svehlova and Poloucek<sup>8</sup>, who found that the impact strength of a filled PP depended on the number of particles (or aggregates arising from poor dispersion during processing) which were  $> 10 \mu\text{m}$ . In addition, in a relatively limited number of cases, information has been presented about the relationship between the size and shape of filler particles and impact strength<sup>9</sup>. On occasion<sup>10</sup>, this information has been related by fracture mechanics studies to the fracture toughness of the composite, with high toughness being thought to be due to retardation of crack propagation by blocking<sup>11,12</sup> or pinning<sup>13,14</sup>, though local plastic deformations are also known to be important in these non-brittle systems<sup>15</sup>.

There are hints that other factors might also be important. In unfilled PP, it is known that changes in micromorphology can affect fracture processes and hence impact strength: examples include modification of spherulite size<sup>16</sup> and changes in the banded morphology which occur as a function of processing conditions<sup>17</sup>. For filled polymers, much less information is available, partly due to the practical difficulties in carrying out optical studies. However, Hutley and Darlington<sup>18</sup> observed a good correlation between the temperature of the onset of crystallization in mineral filled PP (clay, talc and carbonate fillers) and impact strength. This correlation was confirmed by Riley *et al.*<sup>19</sup> for a range of carbonate fillers.

The present study was intended to build on these observations. The nucleation of crystallization in filled PP was studied. The microstructures of the composites

\*To whom correspondence should be addressed

**Table 1** Physical data for mineral fillers and compounding and moulding conditions

Filler	Wt%					Surface area (m <sup>2</sup> g <sup>-1</sup> )
	>20	>10	>5	<2	<1 μm	
Carbonate (C1)	0.01	0.1	0.2	86.0	50.0	6
Carbonate (C2)	-	-	1.8	89.0	71.8	8
Talc (T1)	1.0	4.5	25.0	26.0	10.0	9

Compounding: Baker Perkins MP2030  
 Screw speed, 400 rev min<sup>-1</sup>  
 Temperature settings  
 Feed zone, 155°C  
 Barrel, 180–200°C  
 Granulation: in line, water bath

Injection moulding: Arburg, 'Allrounder' 221-55-250  
 Zone temperatures, 190–225°C  
 Mould temperature, 55°C

were also investigated. The data have been considered in relation to the impact strengths of the filled materials. Fillers used were talc and calcium carbonate, the latter being uncoated or coated with 1% stearic acid.

**EXPERIMENTAL**

Two PP homopolymers were used for the majority of this study: GW522M homopolymer from ICI and T30S from Himont. Some work was also carried out using GW611M copolymer from ICI. Particle size and other data for the mineral fillers are given in *Table 1*. Compounding was carried out on a Baker-Perkins MP2030 twin screw compounding extruder. After granulation and drying, compounds were injection moulded using an Arburg 'Allrounder' 221-55-250 machine. Again, processing data are summarized in *Table 1*. Specimens were stored for at least 5 days at 21°C to allow for relaxation of thermal stresses before mechanical testing was carried out. Unnotched impact tests were carried out on a Yarsley instrumental falling weight impact tester, whilst notched data were collected using moulded Charpy bars on a Monsanto plastic impact machine.

For crystallization work, a Reichart-Jung polyvar optical microscope was used with a Linkham THM 600 hot stage and a PR600 controller. Images were collected using a monochrome video camera with a Chalnicon tube and were recorded on a Hitachi video recorder. D.s.c. studies utilized a Perkin-Elmer DSC-7 instrument; temperature calibration employed an indium standard. X-ray diffraction data were collected from 12 to 30° (2θ) using Cu Kα radiation and a Philips PW1050 vertical diffractometer.

Fracture mechanics experiments were carried out using Charpy-like specimens on the Monsanto plastic impact machine. A cobalt steel cutting tool with a tip radius of 15 μm was used to make notches of various depths in bars of the polymer.

**RESULTS AND DISCUSSION**

*Impact properties*

Information on the impact strength of PP filled with coated and uncoated carbonates and talc is given in *Figures 1* and *2*. If we consider carbonates first, we note that the notched (Charpy) impact strength falls off very

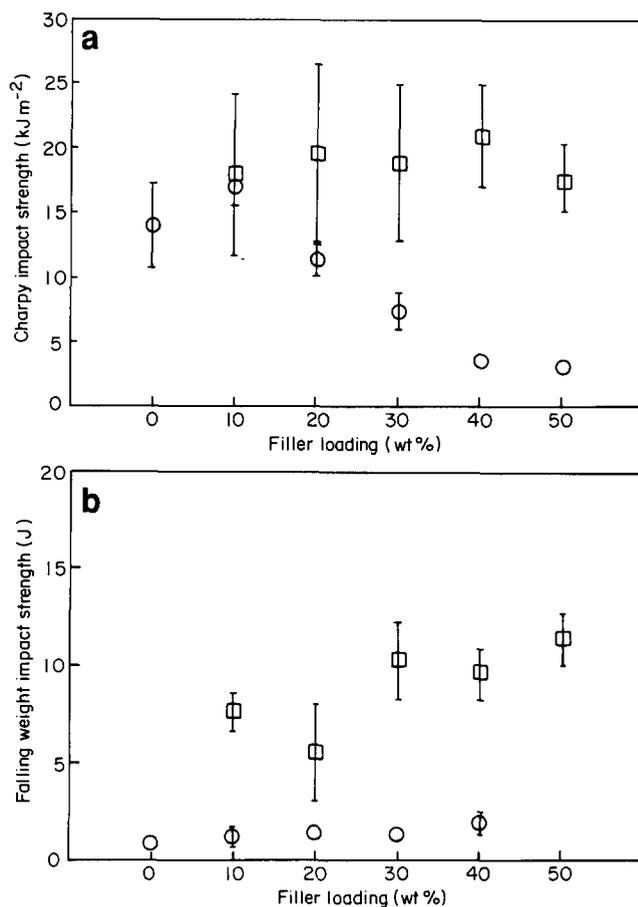


**Figure 1** Effect of stearic acid addition on (a) Charpy and (b) falling weight impact strength for uncoated (O) and stearate-coated (□) carbonate C2 in Himont T30S homopolymer

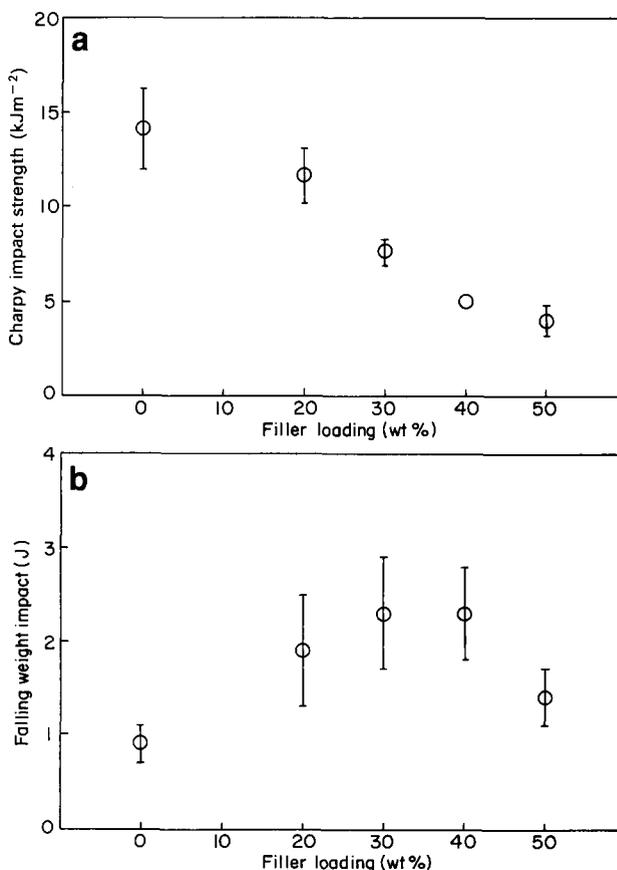


**Figure 2** Effect of filler loading on (a) Charpy and (b) falling weight impact strength for talc T1 in Himont T30S homopolymer

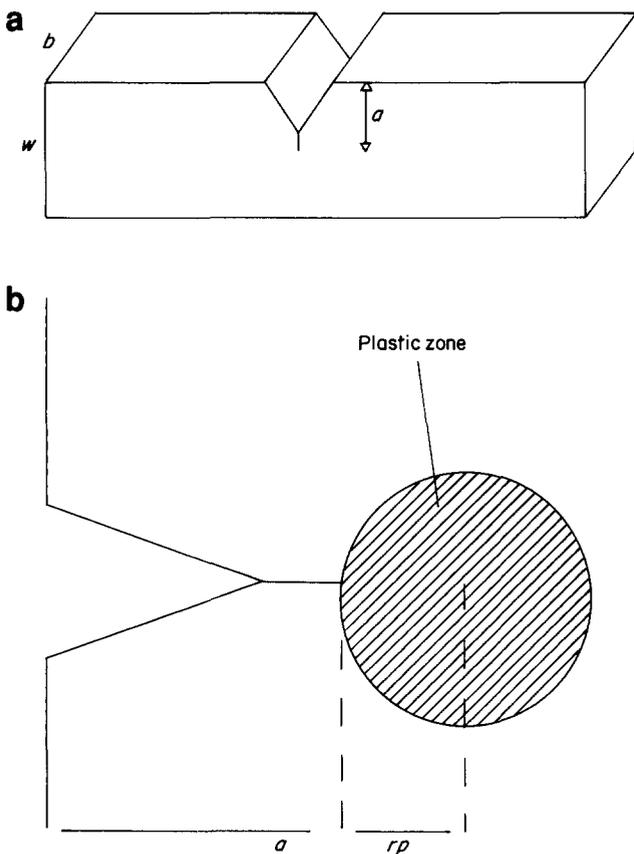


**Figure 3** (a) Geometry of samples used for fracture mechanics studies. (b) Plastic zone model of Irwin<sup>22</sup>. Effective crack length =  $a + r_p$

quickly with the filler loading level ( $> \sim 10$  wt%) for the uncoated filler (C1). However, the coated carbonate shows very different results: the notched impact strength remains high even up to 40 wt% loading. This behaviour is reminiscent of that observed previously by Stanford and Bentley<sup>10</sup>. Differences in falling weight impact strength (FWIS) are even more striking, with an order of magnitude difference between the impact strengths given by the coated and uncoated fillers. It should also be noted that the coated carbonate gives a notched impact strength which is greater than that of the unfilled polymer itself, while the unnotched falling weight impact strength is an order of magnitude greater than that of the unfilled PP. This is truly remarkable since an increase in stiffness in a filled polymer is normally associated with a decrease in impact strength. Use of the stearate-coated carbonate filler improves both stiffness and impact strength concurrently.

The behaviour of talc is also interesting. It is widely accepted that talc behaves 'normally', i.e. as a result of its platy nature, talc enhances stiffness even more than a carbonate filler, but it also degrades impact properties. This is certainly the case for notched impact strength (Figure 2a), but is not so for FWIS (Figure 2b). Here, though the effect is not as large as that seen for coated carbonate, the impact strength is greater than that of the unfilled PP and remains so until at least 40 wt% loading.

#### Fracture mechanics

A method for determining the critical strain energy release rate,  $G_c$ , a measure of fracture toughness, from impact tests using linear elastic fracture mechanics has been described by Kinloch and Young<sup>20</sup>. The method

involves the measurement of impact energy as a function of notch size for Charpy-like specimens with sharp notches (Figure 3). The impact energy is related to the geometry of the sample by:

$$U_{\text{mes}} - U_{\text{Ke}} = G_c b w Z$$

where  $U_{\text{mes}}$  is the measured impact energy and  $Z$  is a geometry-dependent calibration factor which has been tabulated by Plati and Williams<sup>21</sup>.  $U_{\text{Ke}}$  is the energy dissipated during impact as kinetic energy: it is determined by repeating the test with two broken halves of the Charpy bar joined loosely together. A plot of  $(U_{\text{mes}} - U_{\text{Ke}})$  versus  $b w Z$  should give a straight line of slope  $G_c$ . Since PP is not a perfectly linear elastic material at the temperatures we are concerned with here ( $\sim 20^\circ\text{C}$ ) such an approach is open to question. However, Irwin<sup>22</sup> showed that provided the region of plastic deformation is small compared with the width of the specimen, then the fracture behaviour can be understood by regarding the crack of length  $a$  as being extended to a length  $a + r_p$ , where  $r_p$  is the radius of the plastic zone (Figure 3b).

Figure 4a shows plots of  $(U_{\text{mes}} - U_{\text{Ke}})$  against  $b w Z$  for carbonate (C1) filled PP (homopolymer and copolymer). In each case the original values of the crack length are used, and it can be seen that there is a positive intercept on the y-axis. Figure 4b shows the effect of increasing  $r_p$ , until the best-fit straight line passes through the origin. The values of  $G_c$  and  $r_p$  thus obtained are shown in Table 2, as are data for PP filled with

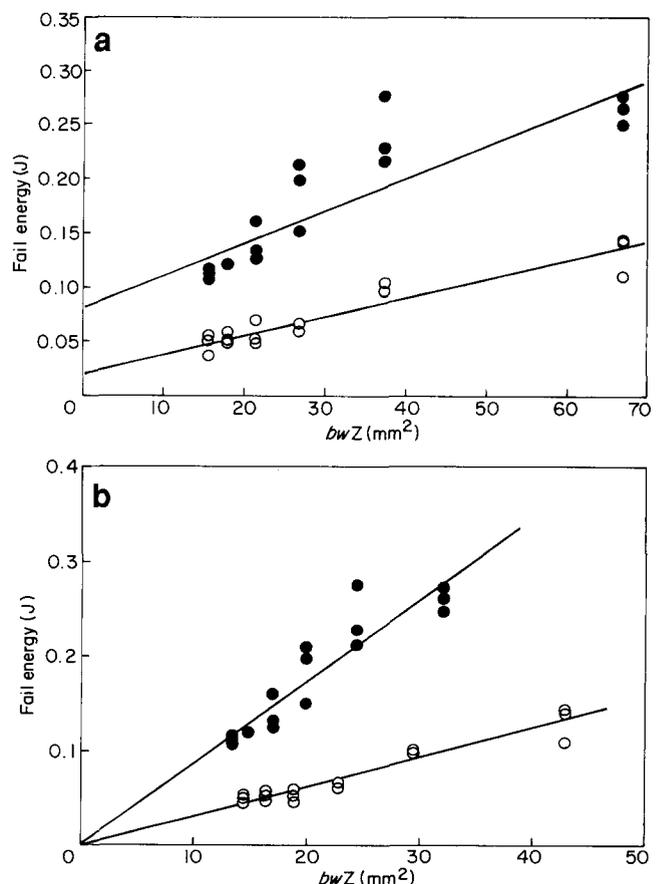


**Figure 4** Plots to determine  $G_c$  in carbonate (C1)-filled PP: (●) homopolymer (GW522M); (○) copolymer (GW601M). In (a) no correction is applied for the plastic zone but in (b) the correction is applied

**Table 2** Fracture toughness

Sample	Charpy impact strength (kJ m <sup>-2</sup> )	G <sub>c</sub> (kJ m <sup>-2</sup> )	r <sub>p</sub> (mm)
Unfilled homopolymer (GW522M)	11.5 ± 1.0	3.2	0.08
Homopolymer 40% filled with C1	9.5 ± 2.0	3.1	0.26
Homopolymer 40% filled with stearate-coated C1	13.0 ± 4.5	5.0	0.31
Unfilled copolymer (GW601M)	23.0 ± 0.6	4.5	0.10
Copolymer 40% filled with C1	26.1 ± 2.5	8.7	0.53
Copolymer 40% filled with stearate-coated C1	32.2 ± 1.8	10.6	0.38

stearate-coated carbonate. Notice that:

1. the plastic zone is larger in the copolymer than in the homopolymer, as might be expected;
2. the values of G<sub>c</sub> follow the same order as the Charpy impact strengths;
3. the value of G<sub>c</sub> for the unfilled homopolymer (3.2 kJ m<sup>-2</sup>) compares well with other values reported in the literature<sup>23–27</sup>, i.e. they lie in the range 2.8–3.0 kJ m<sup>-2</sup>. Values for PP copolymers are difficult to compare, since there is such a wide range of materials under this name. For example, G<sub>c</sub> values of 3.86 (ref. 26) and 9.50 (ref. 27) have been reported for 'PP copolymers'.

Stanford and Bentley<sup>10</sup> have reported r<sub>p</sub> values of 0, 0.2 and 0.7 mm, respectively for unfilled, carbonate-filled and stearate-coated carbonate-filled PP homopolymer. The values found in this study are of the same order of magnitude, and the differences are probably due to differences in the filler and the grade of PP.

#### Nucleation/crystallization

The isothermal nucleation of crystallization and the growth of spherulites was observed in unfilled PP by optical microscopy. Samples were annealed for 10 min at 230°C before being cooled quickly to the temperature of study. It can be seen (Figure 5a) that at every temperature studied, the growth rate of the spherulites was constant with time; the rate also increased rapidly at lower crystallization temperatures (Figure 5b). In a study of carbonate-filled PP, Kowaleski and Galeski<sup>26</sup> demonstrated that the filler had no measurable effect on the spherulitic growth rate. This was confirmed in the present study using samples containing small (2 wt%) quantities of filler (at higher loading levels, it was difficult to see spherulitic structure). It would appear then, that differences in crystallization behaviour between different fillers must be due to differing capacities for nucleation of crystallization.

The crystallization behaviour of filled PP was studied by d.s.c. Once again, the samples were annealed at 230°C for 10 min before cooling at 200°C min<sup>-1</sup> to the crystallization temperature. Typical traces, showing the effect of increasing filler levels, are shown in Figure 6. Traditionally, data of this type have been treated by use of the Avrami equation<sup>28</sup>. Very often, two regions of different slope are seen, the first due to primary nucleation, and the second due to modification of the

spherulites, i.e. increasing the crystalline perfection. In general, though not invariably, the Avrami plots produced here showed evidence of both primary and secondary regions (e.g. Figure 7). The major difference seen, however, was in the Avrami exponent, *n*. For talc, in the primary nucleation region, *n* was ~3, whereas with carbonate *n* was lower at ~2.2–2.5. With the stearate-coated filler, the slope was yet lower (~1.5–2.0). The underlying physical origin of the differences in *n* is

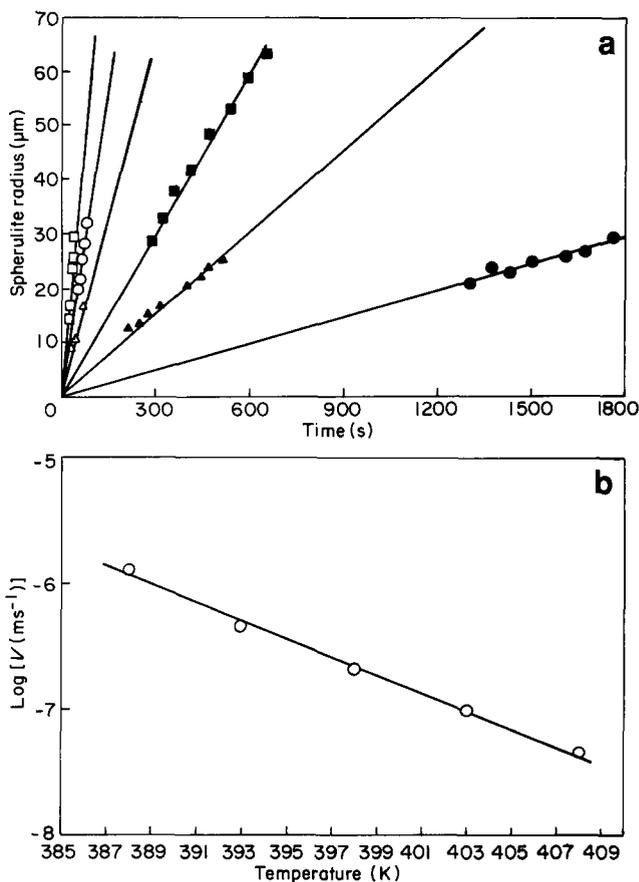


**Figure 5** (a) Spherulite radius versus time for unfilled PP homopolymer (GW522M): (□) 115°C; (○) 120°C; (△) 125°C; (■) 130°C; (▲) 135°C; (●) 140°C. (b) Dependence of spherulite growth rate on temperature

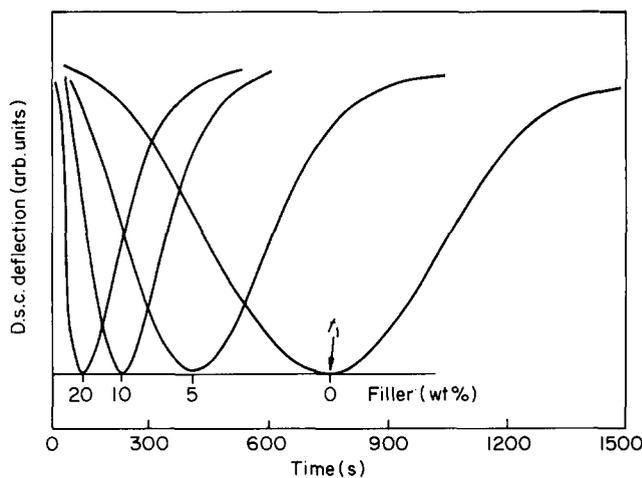


**Figure 6** D.s.c. data for PP homopolymer (GW522M) filled with carbonate C1 at different loadings

not completely clear. Non-integral values of  $n$  have been assigned variously to *inter alia* secondary crystallization processes<sup>29,30</sup>, mixed nucleation modes<sup>31</sup> and changes in the radial density of the crystallizing units<sup>32</sup>. We may simply deduce that crystallization behaviour depends upon the type of filler used.

Further information was also obtained from the d.s.c. data using an analytical model plus a computer model related to, but rather simpler than that of Galeski<sup>33</sup>. The analytical model is essentially two-dimensional, with  $N_A$  nucleating sites per unit area arranged in regular hexagonal close packing. It is assumed that all nucleation occurs at time  $t_0$  and that spherulites grow unhindered at a rate equal to that seen in the unfilled polymer. When the leading edges of adjacent spherulites touch, it is

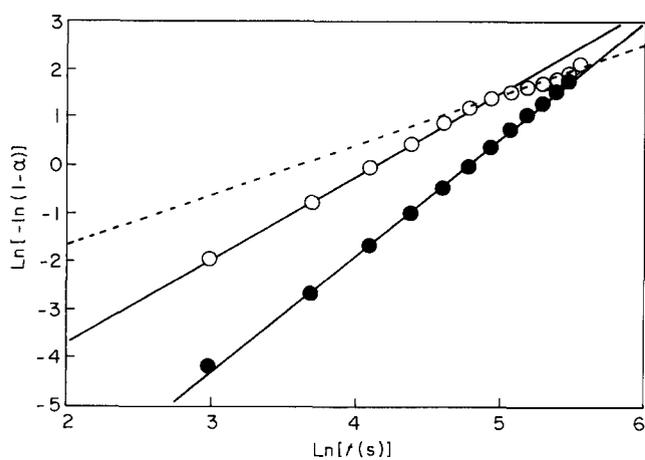


Figure 7 Avrami plots for crystallization of PP filled with uncoated (●) and coated (○) C1 carbonate at 135°C

assumed that crystallization stops at points of contact, but continues elsewhere at the same rate. It can be shown (see Appendix) that

$$N_A^{\max} = [2\sqrt{3}(dr_0/dt)^2 t_1^2]^{-1}$$

where  $dr_0/dt$  is the unhindered radial growth rate of spherulites and  $t_1$  is the time to reach the turning point (the maximum deflection) of the d.s.c. curve.

Hexagonal packing is the optimal scheme in two dimensions. Thus for a given  $t_1$ , the value of  $N_A^{\max}$  derived from this expression represents the largest possible value.

In reality, nucleating sites are not regularly distributed, and a computer simulation was used to model the spherulite growth (still in two dimensions) from a random distribution of nucleating sites. The program was used iteratively, with  $N_A^{\max}$  as an initial value, to derive refined values for  $N_A$  corresponding to observed values of  $t_1$  and  $dr_0/dt$ . The number of nucleating sites per unit volume was assumed to be given by  $N_A^{1.5}$ .

If account is taken of the surface areas of the fillers used (Table 1), it is possible to derive (see Appendix) the number of nucleating sites per unit area of the mineral surface ( $N_f$ ). Values in the range  $10^7$ – $10^{10}$   $m^{-2}$  were found at crystallization temperatures of 135°C, i.e. talc  $\sim 3 \times 10^9$ , carbonate  $\sim 6 \times 10^7$ , stearate-coated carbonate  $\sim 3 \times 10^7$   $m^{-2}$ . The values are critically dependent not only on the filler type, but also on temperature (Table 3).

The reason for the very high nucleation activity of talc has not been fully elucidated. However, the nucleating ability has been associated with the small radius features such as steps, notches, dislocations, edges, etc.<sup>34</sup>. Certainly, with the similar platey silicate filler mica, it has been demonstrated that nucleation occurs at the flake edges<sup>35</sup>.

Table 3 Number of nucleating sites per surface area of filler

Sample	$t_m$ (min)			$N_A$ ( $\times 10^7$ $m^{-2}$ ) <sup>a</sup>			No. of nucleating sites per surface area of filler, $N_f$ ( $\times 10^6$ $m^{-2}$ )		
	130°C	135°C	140°C	130°C	135°C	140°C	130°C	135°C	140°C
Unfilled homopolymer (GW522M)	4.7	12.2	33.3	30	16	20	–	–	–
Homopolymer filled with C1 carbonate									
5 wt%	2.3	6.7	23.2	90	40	40	78	22	19
10 wt%	1.5	3.7	11.7	160	145	80	102	92	34
20 wt%	1.3	3.2	10.5	195	190	190	127	65	64
Homopolymer filled with stearate-coated C1 carbonate									
5 wt%	2.4	6.8	25.8	75	40	36	55	22	14
10 wt%	1.9	4.9	16.3	130	75	71	72	32	28
20 wt%	1.4	3.4	11.2	300	180	160	65	60	49
Unfilled homopolymer (GW522M batch 2)	–	11.3	–	–	22	–	–	–	–
Homopolymer filled with T1 talc									
5 wt%	–	1.2	–	–	1300	–	–	3530	–
10 wt%	–	0.9	–	–	2000	–	–	2800	–
20 wt%	–	0.9	–	–	2000	–	–	1300	–

<sup>a</sup>See Appendix

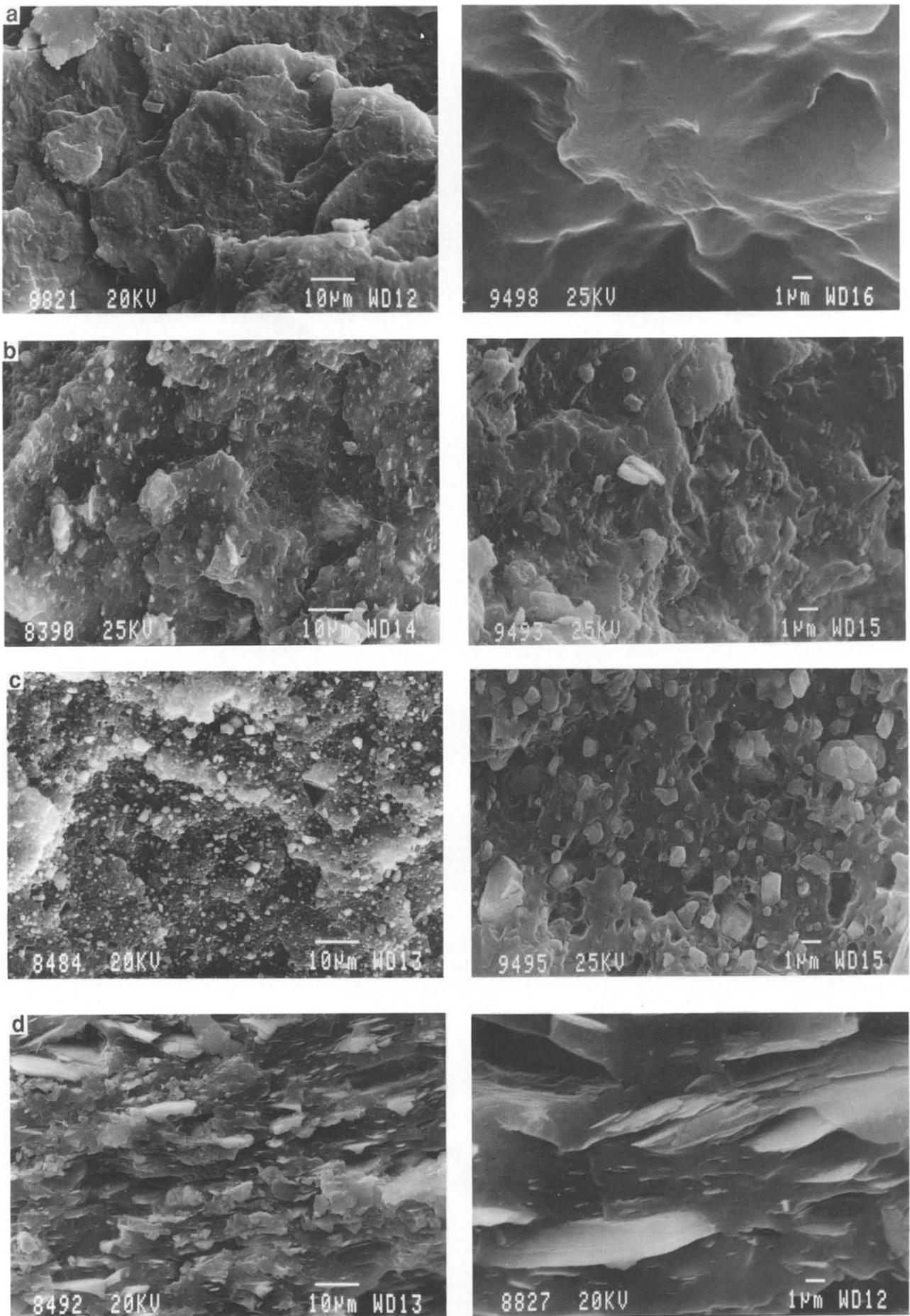


**Figure 8** Scanning electron micrographs of Charpy-fracture surfaces in PP. (a) Unfilled, and filled with (b) C1 carbonate, (c) coated C1 carbonate and (d) talc T1

**Table 4** Crystallinity data

Crystallinity data for filled and unfilled PP homopolymer (GW522M) <sup>a</sup>						
Sample	D.s.c.	I.r.	C	C <sup>1</sup>	B	A
Unfilled PP	60	68	3.7	3.4	0.055	0.88
PP + carbonate C1 (40 wt%)	59	66	3.6	2.8	0.065	0.80
PP + stearate- coated C1 (40 wt%)	60	68	4.0	2.5	0.120	0.83
PP + talc (40 wt%)	55	–	11.5	10.6	0.018	0.92

Variation of  $\beta$ -phase index in PP mouldings filled (40 wt%) with stearate-coated carbonate C1

Distance from gate (cm)	C
1.3	0.118
2.3	0.092
2.8	0.128
3.7	0.146
4.8	0.096
5.7	0.063
6.6	0.122
7.5	0.086
8.6	0.101

<sup>a</sup>D.s.c., i.r., percentage crystallinity from d.s.c. and i.r. studies; C, crystallinity index; C<sup>1</sup>, crystallinity index after removal of surface layer; B,  $\beta$ -phase index; A, orientation index of  $\alpha$ -phase

### Micromorphology

A variety of methods were used for characterization of polymer microstructure. The first requirement was to ascertain whether all of the fillers were well dispersed in the polymer matrix; if this were not the case, Griffith fracture would dominate the impact results. It can be seen (Figure 8), that in all of the filled samples, the filler particles were dispersed evenly: there was no evidence of aggregates. In addition, several other points of interest are evident in the micrographs in Figure 8. First, it can be seen that in the case of the talc-filled system, the talc plates are aligned almost parallel to each other. Second, for PP filled with uncoated carbonate or talc, there appears to be good bonding between the filler and the polymer. Third, in contrast, the particles of the stearate-coated carbonate are very poorly bonded to the polymer; holes can be seen in the polymer surface where filler has 'fallen out' during fracture.

Both d.s.c. and i.r. methods were used to obtain the percentage crystallinity. In addition, the crystallinity index, the  $\beta$ -phase index and the  $\alpha$ -phase orientation index (as defined by Turner-Jones *et al.*<sup>27</sup>) were derived from X-ray diffraction data (Table 4). In all cases, the percentage crystallinity was approximately constant (55–70%). This is in agreement with previous results obtained with carbonate-filled PP<sup>12</sup>. Extremely noteworthy is the very high crystallinity index obtained with talc-filled compounds. Also of importance is that there are some differences between measurements made before and after removal of the surface layer (150  $\mu$ m) from mouldings by abrasion (Table 4). In all cases, the crystallinity of the core is slightly lower than that near the surface, most significantly so in the case of the PP filled with stearate-coated carbonate.

Other information is also available from X-ray diffraction (Table 4). Notable differences were found in

the amount of  $\beta$ -phase crystallites in the different polymer samples. In particular, talc-filled samples have very low  $\beta$ -phase indices (0.02) whereas for unfilled and carbonate-filled polymer, the index was  $\sim$ 0.06. The index was very much higher in polymer filled with stearate-coated carbonate. Interestingly, and in contradiction to data produced recently for unfilled PP<sup>17</sup>, the  $\beta$ -phase index is constant and high right across the moulding (Table 4). (It is worth stressing here that the  $\beta$ -phase index is an arbitrary measure, derived from X-ray diffraction data. An index of 0.1 certainly implies more  $\beta$ -phase than an index of 0.05, but an index of 0.1 does not imply that 10% of the crystalline polymer is in the  $\beta$  form.)

### Relationship of nucleation, crystallization and microstructure to impact strength and fracture toughness

If we summarize the experimental data given in Figures 1 and 2, and simplify the picture by considering only 40 wt% filled polymers we see that:

for notched (Charpy) impact strengths  
coated carbonate > unfilled > carbonate = talc  
for unnotched (falling weight) impact strengths  
coated carbonate > carbonate = talc > unfilled

The effects produced by the different fillers are extremely significant. In the case of unnotched impact, the range in impact strengths covers a factor of 5. Differences in FWIS are even more striking, with an order of magnitude difference between the impact strengths given by the coated and uncoated carbonate fillers. Indeed, the stearate-coated carbonate gives an order of magnitude improvement not only over the uncoated carbonate and talc-filled PP, but also over the unfilled polymer itself, a very dramatic result. We need to understand the factors which are important in producing this pattern.

Judging by the (admittedly qualitative) electron micrograph evidence (Figure 8), it does not appear that there are any significant problems of dispersion of any of the fillers into the PP matrix. Failure due to the presence of large agglomerates does not seem likely.

The relative impact strength values are undoubtedly related to the ability of different fillers to pin or block cracks<sup>4,5,12,19</sup>. In all of the filled systems studied here, the sizes of the filler particles are of the same order of size as, or larger than, the tips of the propagating cracks (estimated by Sims<sup>36</sup> to be of the order of 0.3–0.5  $\mu$ m). In line with these ideas, the fracture toughness, i.e.  $G_c$  values, derived from the fracture mechanics studies, were much greater than those of the unfilled polymer (Table 2).

In a recent publication, Nezbedova *et al.*<sup>9</sup> presented data for PP filled with uncoated calcium carbonates of different types. They showed that the addition of filler modifies the toughness depending upon concentration, particle size and test temperature. Below  $\sim$ 25 wt% filler, they found that use of a filler with a very small particle size ( $\sim$ 0.5–2  $\mu$ m, precipitated carbonate) gave rise to higher toughness at all temperatures, while with ground carbonates (larger particles of  $\sim$ 5  $\mu$ m), the increase in toughness only occurred below the tough/brittle transition temperature of the polymer matrix. It was suggested that addition of carbonate influences the energy absorbed in two different ways. First, an increase in toughness occurs due to additional shear deformation of the matrix around the filler particles, especially near the fracture initiation site, and second, a reduction in

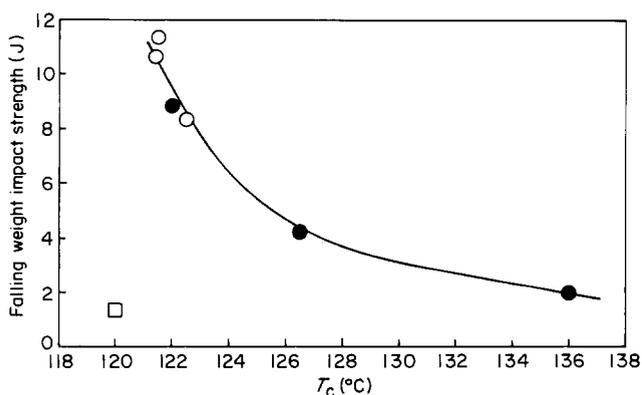


Figure 9 Dependence of impact strength on the temperature of the onset of crystallization,  $T_c$ : (○) coated carbonate; (●) uncoated carbonate; (□) unfilled PP

toughness due to reduced plastic flow in the PP matrix. In the present work it was observed (Figure 8) that there were major differences in the fracture processes which occur on addition of filler and, indeed between fillers. Moreover,  $G_c$  values, and the radii of the plastic zones, were seen to be much larger for the filled than unfilled systems, especially for PP filled with stearate-coated carbonate. Also, in the case of the stearate-coated carbonate, impact strength could be enhanced by the energy required to 'pull particles out' of the inclusions in the polymer in which they are situated. Clearly this mechanism cannot operate where there is no filler, or where there is good filler-matrix bonding (e.g. talc, uncoated carbonate).

If we consider talc fillers, we can identify two features on electron micrographs which are probably related to the relatively low impact strengths of talc-filled composites. Firstly, the talc platelets are arranged parallel to each other in the compound. This information was originally accessed through X-ray diffraction by Rybnikar<sup>37</sup>. He also demonstrated that the growth of PP on the talc surface was epitaxial, with PP tending to crystallize with  $a, c$  planes being parallel to the  $a, b$  planes in talc. Such alignment would probably mean that crack propagation would be anisotropic, i.e. rather easier parallel to the talc plates than perpendicular to them due to a reduction in crack pinning or blocking. Secondly, the talc particles have very sharp edges, potential sites for high stress concentrations<sup>19</sup> when the composites are deformed.

While those mechanical features are undoubtedly important – they can be invoked to explain why the impact strength of filled PP exceeds that of the unfilled polymer and why the impact strength of carbonate-filled polymer is greater than that of the talc-filled polymer – they cannot explain the direct correlation between crystallization behaviour (specifically the temperature of the onset of crystallization,  $T_c$ ) and impact strength observed by Hutley and Darlington<sup>18</sup> and Riley *et al.*<sup>19</sup> (see Figure 9). Moreover (unless we are being misled about the presence of aggregates by the electron micrographic data), the fracture mechanics approach cannot explain why the impact strength of PP filled with coated carbonate is much greater than that when uncoated carbonate is used.

In essence, we need to explain why coated carbonates have low  $T_c$  values and high impact strength, while uncoated carbonates have high  $T_c$  and low impact

strength. The fact that talc has a very high  $T_c$  and a low impact strength may also be relevant, but other reasons for the relatively poor impact performance of talc-filled PP have already been indicated above.

In simplistic terms, it might be argued that a filler with good nucleating properties would give a high onset temperature and a large number of nuclei per unit volume. This would imply a fine spherulite morphology and, hence, by analogy with unfilled polymer<sup>16</sup>, good impact strength. That this simple argument is not correct is easily seen: it predicts an opposite trend to that observed<sup>18,19</sup>. The approach might well be flawed; it is not obvious, for example, that lower temperature nucleation would lead to larger spherulites.

If we consider the possible effects on the polymer microstructure which might result from using a nucleating or non-nucleating filler, we note that at certain crystallization temperatures, growth of  $\beta$ -phase crystallites is relatively favoured. For example, Lovinger *et al.*<sup>38</sup> showed that between 122°C and 138°C, the  $\beta$ -phase grows at a rate which is 20–70% faster than the  $\alpha$ -phase, with the difference in growth rates being greatest at low temperatures. Now, this is just the temperature regime of interest. It can be seen (Figure 9), that  $T_c$  values for uncoated carbonates are at the upper end of this range, while coated carbonates are near the lower temperature limit. In accordance with this information, we note (Table 2) that the  $\beta$ -phase index for PP filled with the coated carbonate is much greater than for the uncoated carbonate. Thus, we see that a major effect on microstructure is one outcome of modification of the nucleating ability of the filler.

There is some confusion concerning the effect of the  $\beta$ -phase. Murphy *et al.*<sup>17</sup> have studied the correlation of mechanical properties and microstructure at different positions in a moulding. They implied that the presence of  $\beta$ -phase polymer reduces the impact strength of unfilled PP. Contrary to this, it has been suggested<sup>39,40</sup> that the presence of  $\beta$ -phase crystallites actually enhances impact strength. Such a suggestion is in accordance with the data presented here.

One anomaly remains to be addressed. Although the  $T_c$  values for both unfilled PP and PP filled with stearate-coated carbonate are much the same (Figure 9), the  $\beta$ -phase indices are very different (Table 4). There are two possible reasons for this: (1) although the onset of nucleation occurs at  $\sim 120^\circ\text{C}$  in both cases, there are more nucleating sites per unit volume of polymer in the filled polymer than in the unfilled; (2) the presence of a filler will influence the rate of cooling during injection moulding. It may be that the effect is to prolong the period during which the cooling polymer is in the temperature region which favours growth of the  $\beta$ -phase. On balance, the first of these explanations seems more likely.

## CONCLUSIONS

In summary, we propose that the following factors contribute to the impact properties of mineral filled PP.

1. Good dispersion of the filler is necessary. Failure to achieve this will result in poor impact strength.
2. Crack pinning and/or blocking will increase the fracture energy  $G_c$  with respect to the unfilled polymer, and thus enhance the impact strength, although the

magnitude of this effect will probably depend upon particle size and shape.

3. 'Particle pull-out' may also enhance impact strength in some cases, and probably contributes to the good impact properties of stearate-coated carbonate filled systems.
4. High stress concentrations in the vicinity of filler particles are likely to be detrimental to impact strength. The magnitude of this stress concentration is large for high aspect ratio particles, and thus platy fillers such as talc are likely to suffer more severely from this effect.
5. The impact strength is further increased when non-nucleating fillers are used, a consequence of crystallization in a temperature region which favours the presence of  $\beta$ -phase crystallites.

## REFERENCES

- 1 'Minerals for Plastics – a European Review', Plastics Consult SRL, Milan, 1984
- 2 Ladawar, G. E. and Beecher, N. *Polym. Eng. Sci.* 1970, **10**, 185
- 3 Lewis, T. B. and Nielsen, L. E. *J. Appl. Polym. Sci.* 1970, **14**, 449
- 4 Nielsen, L. E. *J. Appl. Phys.* 1970, **41**, 4726
- 5 Chow, T. S. *J. Mater. Sci.* 1980, **15**, 1873
- 6 Farker, J. N. and Farris, R. J. *J. Appl. Polym. Sci.* 1987, **34**, 2093
- 7 Griffith, A. A. *Phil. Trans. R. Soc.* 1920, **A221**, 163
- 8 Svehlova, V. and Poloucek, E. *Angew Makromol. Chem.* 1987, **153**, 197
- 9 Nezbedova, E., Ponesicky, J. and Sova, M. *Acta Polym.* 1990, **41**, 36
- 10 Stanford, J. and Bentley, S. R. 'Filplas '89' – The Fillers Conference', PRI, London, 1989, paper 18
- 11 Cook, J. and Gordon, J. E. *Proc. R. Soc.* 1964, **A282**, 508
- 12 Vollenberg, P. H. Th. *PhD Thesis* Technische Universitat Eindhoven, 1987
- 13 Green, D. S., Nicholson, P. S. and Emburg, J. D. *J. Mater. Sci.* 1979, **14**, 1413
- 14 Green, D. G., Nicholson, P. S. and Emburg, J. D. *J. Mater. Sci.* 1979, **14**, 1657
- 15 Kinloch, A. J., Maxwell, D. L. and Young, R. J. *J. Mater. Sci.* 1985, **20**, 4169
- 16 Friedrich, K. *Progr. Colloid. Polym. Sci.* 1978, **64**, 103
- 17 Murphy, M. W., Thomas, K. and Bevis, M. *J. Plast. Rubber Proc. Appl.* 1988, **9**, 3
- 18 Hutley, T. J. and Darlington, M. *Polym. Commun.* 1985, **26**, 264
- 19 Riley, A. M., Paynter, C. D., McGenity, P. M. and Adams, J. M. *J. Plast. Rubber Proc. Appl.* 1990, **14**, 85
- 20 Kinloch, A. J. and Young, R. J. 'Fracture Behaviour of Polymers', Elsevier, London, 1983
- 21 Patti, E. and Williams, J. G. *Polym. Eng. Sci.* 1975, **15**, 470
- 22 Irwin, G. R. *Appl. Mater. Res.* 1964, **3**, 65
- 23 Coppola, F., Greco, R. and Ragosta, G. *J. Mater. Sci.* 1986, **21**, 1775
- 24 Levita, G., Marchetti, A. and Lazzeri, A. *Polym. Composites* 1989, **10**, 39
- 25 Chen, L. S., Mai, Y. W. and Cotterell, B. *Polym. Eng. Sci.* 1989, **29**, 505
- 26 Kowaleski, T. and Galeski, A. *J. Appl. Polym. Sci.* 1986, **32**, 2919
- 27 Turner-Jones, A., Aizlewood, J. M. and Beckett, D. R. *Makromol. Chem.* 1964, **75**, 134
- 28 Alfonso, G. C., Pedemonte, E., Re, M. and Turturro, A. *Gazz. Chem. Ital.* 1982, **112**, 99
- 29 Hay, J. N. *Br. Polym. J.* 1971, **3**, 74
- 30 Hay, J. N. *J. Polym. Sci., Polym. Lett. Edn* 1976, **14**, 543
- 31 Sharples, A. *Polymer* 1962, **3**, 250
- 32 Hay, J. N. and Przekop, Z. *J. Polym. Sci., Polym. Phys. Edn* 1979, **17**, 951
- 33 Galeski, A. *J. Polym. Sci., Polym. Phys. Edn* 1981, **19**, 721
- 34 Binsberger, F. L. *J. Polym. Sci., Phys. Edn* 1973, **11**, 117
- 35 Thapar, H., Hornsby, P. R., Folkes, M. J. and Bevis, M. J. personal communication
- 36 Sims, G. L. A. *J. Mater. Sci.* 1975, **10**, 647
- 37 Rybnikar, F. *J. Appl. Polym. Sci.* 1989, **38**, 1479
- 38 Lovinger, A. J., Chua, J. O. and Gryte, C. C. *J. Polym. Sci.,*

*Polym. Phys. Edn* 1977, **15**, 641

39 Kathen, W. *Ger. Offen. DE 3 443 599 A1*, 1986

40 Shi, G., Zhang, J. and Jin, H. *Ger. Offen. DE 3 610 544*, 1986

## APPENDIX – MODEL FOR CRYSTALLIZATION

### Regular two-dimensional lattice model

Consider a two-dimensional film of polymer containing  $N_A$  nucleating sites per unit area, arranged regularly in hexagonal close packing, each a distance  $d$  from its immediate neighbours (Figure A1). Assuming that spherulite growth commences at the same instant at each nucleating site and that no other nucleation occurs, there will be three distinct periods of spherulite growth (let  $\theta$  = area fraction of polymer crystallized, and  $r(t)$  = spherulite radius at time  $t$ ):

1. at time  $t_0$  (start of crystallization) spherulites will grow unhindered at a radial rate  $dr_0/dt$ . The rate of crystallization,  $d\theta/dt$  is proportional to  $r(t)$ .
2. At time  $t_1$ , when  $r = d/2$ , the leading edges of adjacent spherulites contact at the nearest point. It is assumed that crystallization stops at points of contact, but continues elsewhere at the rate  $dr_0/dt$ . The rate of crystallization slows down and is a function of the area of polymer remaining uncrystallized. Crystallization is assumed to be complete within the spherulite boundary.
3. At time  $t_2$ , the polymer is completely crystallized and  $d\theta/dt = 0$ .

On the d.s.c. curves for isothermal crystallization, the rate of heat output is proportional to  $d\theta/dt$ . Thus, the time at which the d.s.c. curve reaches a turning point is the same for  $d\theta/dt$  to reach a turning point, i.e.  $t = t_1$ . The number of nucleating sites per unit area,  $N_A$ , is simply related to the time  $t_1$  by:

$$N_A = [2\sqrt{3}(dr_0/dt)^2 t_1^2] \quad (\text{A1})$$

The time  $t_1$  is read directly off the d.s.c. curve; the spherulite radial growth rate,  $dr_0/dt$  is obtained from optical microscopy and therefore  $N_A$  is determined. Hexagonal close packing is the optimal two-dimensional packing scheme, hence, for given values of  $t_1$  and  $dr_0/dt$ , the value of  $N_A$  derived from equation (A1) will be the maximum possible value, henceforth denoted  $N_A^{\text{max}}$ .

### Two-dimensional computer model

In reality, nucleating sites will not be regularly distributed throughout the polymer, but will be scattered randomly. A computer program was written to model

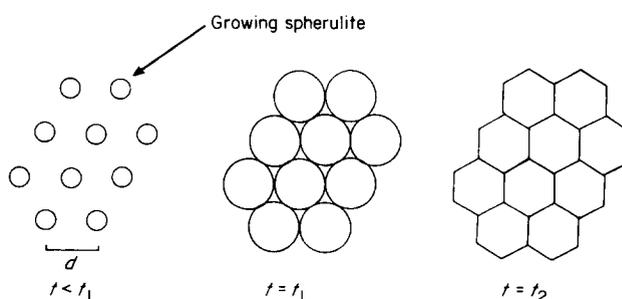
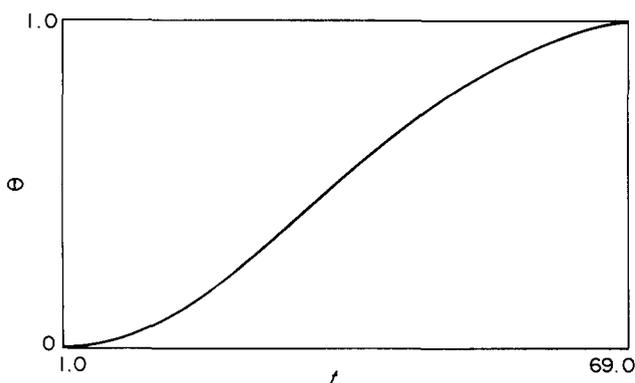
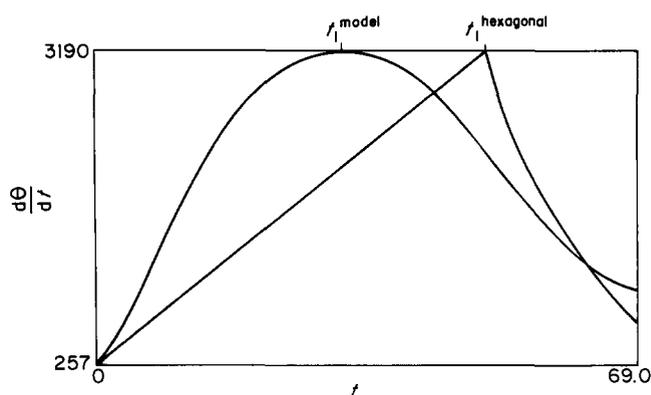


Figure A1 Diagram of spherulite growth in the highly idealized situation of hexagonal packing



**Figure A2** A plot of  $\theta$  versus  $t$  for spherulite growth originating from a random distribution of nucleating sites. In this particular example,  $t = 69$  s corresponds to the polymer being 90% crystallized



**Figure A3** Plots of  $d\theta/dt$  versus  $t$  for a given value of  $N_s$ . The curve peaking at  $t_1^{\text{model}}$  is obtained by numerically differentiating and smoothing the curve shown in *Figure A2*. The curve with the sharp peak at  $t_1^{\text{hexagonal}}$  is that predicted by the idealized hexagonal packed model

the two-dimensional growth of spherulites with a random distribution of nucleating sites, the effect of which is to 'blur' the turning point  $t_1$ . Because random packing is less efficient than hexagonal packing, for a given  $N_A$ ,  $t_1$  (random)  $<$   $t_1$  (hexagonal) (*Figure A1*). Consequently, for a given  $t_1$ ,  $N_A$  (random)  $<$   $N_A$  (hexagonal).

The computer model calculated the area fraction of polymer crystallized,  $\theta$ , as a function of time. Parameters such as  $N_A$ ,  $dr_o/dt$  and the mesh size of the cartesian grid used in the numerical model of spherulite growth were specified at the start of the program. *Figure A2* illustrates a typical  $\theta$  versus  $t$  curve. These data were numerically differentiated and smoothed to yield the  $d\theta/dt$  versus  $t$  curve, from which  $t_1$  may be obtained (cf. with the prediction of the simple theory outlined in the previous section; *Figure A3*).

The shape of the  $d\theta/dt$  versus  $t$  curve from the computer model is much broader than the theoretical curve; this is to be expected, since with the random distribution of nucleating sites, some will be much closer together than expected from the regular spatial arrangement of the theory, and similarly, others will be further apart.

Values for  $t_1$  were obtained from the d.s.c. experiments (denoted  $t_1^{\text{DSC}}$ ) and together with the values of  $dr_o/dt$  determined by optical microscopy, used to determine  $N_A^{\text{max}}$  by equation (A1).  $N_A = N_A^{\text{max}}$  was used as an initial value in the computer simulation and a corresponding value for  $t_1$  obtained and denoted  $t_1^{\text{model}}$ . The values of  $N_A$  were then adjusted iteratively until  $t_1^{\text{model}} = t_1^{\text{DSC}}$ .

*Extrapolation to three dimensions and derivation of nucleating sites per unit area of filler*

The number of nucleating sites per unit volume was identified as  $N_A^{1.5}$ . From this value, after subtraction of an appropriate fraction of the  $N_A^{1.5}$  value of the unfilled polymer, the number of nucleating sites per unit surface area of the filler,  $N_f$ , was calculated from a knowledge of the filler loading, the densities of PP ( $0.9 \text{ g cm}^{-3}$ ) and the fillers ( $\sim 2.6 \text{ g cm}^{-3}$  for both talc and calcium carbonates) and the nitrogen surface areas of the fillers (*Table 3*).